



Distribution of trace and major elements in subarctic ecosystem soils: Sources and influence of vegetation

Yannick Agnan^{a,*}, Romain Courault^b, Marie A. Alexis^a, Tony Zanardo^a, Marianne Cohen^b, Margaux Sauvage^c, Maryse Castrec-Rouelle^a

^a Sorbonne Université, CNRS, EPHE, UMR METIS, F-75252 Paris, France

^b Sorbonne Université, CNRS, FRE ENeC, F-75006 Paris, France

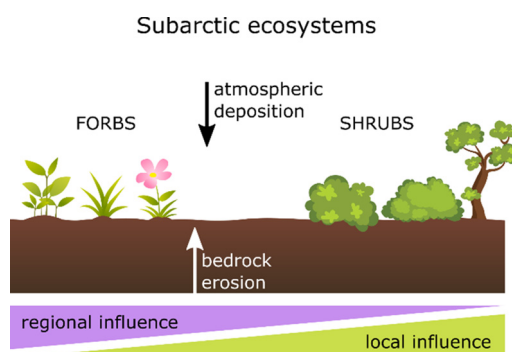
^c Université Paris Diderot, Pôle Image, F-75013 Paris, France



HIGHLIGHTS

- Concentrations of elements were measured in different subarctic soils.
- Four ecosystems were compared: grassland, moor, broad-leaved forest, and peat bog.
- Spatial heterogeneity of concentrations resulted from different sources.
- Only forbs and shrubs showed covariance with trace element distribution.
- Soil pH controlled the geochemical dynamics of As, Cu, and Se.

GRAPHICAL ABSTRACT



ARTICLE INFO

Article history:

Received 17 January 2019

Received in revised form 1 May 2019

Accepted 13 May 2019

Available online 17 May 2019

Editor: F.M. Tack

Keywords:

Trace elements

Soil

Ecosystem

Vegetation

Subarctic

Sources

ABSTRACT

Arctic and subarctic environments are particularly sensitive to climate change with a faster warming compared to other latitudes. Vegetation is changing but its role on the biogeochemical cycling is poorly understood. In this study, we evaluated the distribution of trace elements in subarctic soils from different land covers at Abisko, northern Sweden: grassland, moor, broad-leaved forest, and peat bog. Using various multivariate analysis approaches, results indicated a spatial heterogeneity with a strong influence of soil horizon classes considered: lithogenic elements (e.g., Al, Cr, Ti) were accumulated in mineral horizon classes and surface process-influenced elements (e.g., Cd, Cu, Se) in organic horizon classes. Atmospheric influences included contamination by both local mines (e.g., Cu, Fe, Ni) and regional or long-range atmospheric transport (e.g., Cd, Pb, Zn). A non-negative matrix factorization was used to estimate, for each element, the contribution of various sources identified. For the first time, a comparison between geochemical and ecological data was performed to evaluate the influence of vegetation on element distribution. Apart from soil pH that could control dynamics of As, Cu, and Se, two vegetation classes were reported to be correlated to geochemical factors: forbs and shrubs/dwarf shrubs probably due to their annual vs. perennial activities, respectively. Since these are considered as the main vegetation classes that quickly evolve with climate change, we expect to see modifications in trace element biogeochemical cycling in the future.

© 2019 Elsevier B.V. All rights reserved.

* Corresponding author.

E-mail address: yannick.agnan@biogeochimie.fr (Y. Agnan).

1. Introduction

Arctic tundra and subarctic taiga cover 16% of the continental surface area. Biological and climate characteristics of these two biomes imply distinct net primary productions (180 and 380 g m⁻² a⁻¹, respectively), suggesting different carbon dynamics (Chapin et al., 2011). The limit between these two biomes, which could be up to 200 km in width, constitutes an important vegetation transition: the tundra–taiga ecotone (Callaghan et al., 2002a). Furthermore, the high latitudes are sensitive to climate change with faster warming compared to the rest of the globe (Acosta Navarro et al., 2016; IPCC, 2013). Increase in air temperature induces a permafrost warming (up to 2 °C in 30 years; Romanovsky et al., 2010) that modifies Arctic and subarctic landscapes (Callaghan et al., 2002b). In parallel, long-term high latitude vegetation records show increasing biomass (i.e., greening) in Arctic and subarctic ecosystems related to climate change (Beck and Goetz, 2011; Ju and Masek, 2016). Ecosystems are currently displacing to the North in response to the rising temperatures (Berner et al., 2013). Long-term observations performed in Siberia from 1910s to 2000s report a boreal shift of about 300–500 m (Shiyatov et al., 2007), despite very complex mechanisms implied on the local scale (Callaghan et al., 2013).

Trace elements are characterized by very low concentrations in the environment (<0.1% in the continental crust). They include various chemical families—metals (e.g., Pb, Cd, and Zn), metalloids (As and Sb), and nonmetals (Se)—which behave differently in the environment in relation to their physicochemical characteristics (Kabata-Pendias, 2010). If some of them are required for many biological activities (such as Cu and Zn), all trace elements present potentially harmful effects on human and ecosystem health in more or less high concentrations (Klassen et al., 2010; Ulrich and Pankrath, 1983). In remote areas, such as Arctic and subarctic regions, trace elements come from two major sources: local bedrock erosion (lithogenic fraction) and atmospheric inputs (atmospheric fraction). Indeed, the low air temperature in polar environments increases the atmospheric deposition of contaminants emitted in temperate latitudes (Law and Stohl, 2007). Environmental archives (peat bogs, lake sediments, and ice cores) showed a recent increase of As, Cd, Cu, Pb, and Zn deposition in the Arctic during the last decades attributed to coal and gasoline combustions promoting accumulation of contaminants in the high latitudes (Evenset et al., 2007; McConnell and Edwards, 2008). Some rare metals (e.g., Pt, Pd, Rh) also indicate a dramatic progression since the 1970s linked to their application in various new technologies (Barbante et al., 2001). Distinguishing anthropogenic from natural sources, however, constitutes a challenge in Arctic and subarctic soils (Halbach et al., 2017). Geochemical tracers such as stable isotopes and rare metals (e.g., Ce, La, and Y) can help to assess each source of trace elements (Agnan et al., 2014; Fedele et al., 2008).

Despite their pristine conditions, polar regions are accumulating contaminants that exposes wildlife to bioaccumulation and biomagnification within trophic levels (AMAP, 2018; Dietz et al., 2000; Tyler et al., 1989). Indeed, data reported in Arctic biota indicate important concentrations in different organisms, which induces direct or indirect health impacts (Gamberg et al., 2005). For example, the increase of some elements in West Greenland caribou, likely linked to atmospheric deposition on lichens, may affect their reproduction functions (Gamberg et al., 2016). Both aquatic and terrestrial ecosystems are therefore subjected to a long-term impact of trace elements, and fauna vulnerability was recently shown to be largely dependent on their habitat (Pacyna et al., 2019).

Trace elements therefore require to be spatially characterized to better constrain both pools and fluxes of elements in polar regions (Nygård et al., 2012; Steinnes and Lierhagen, 2018). This is particularly critical in ecosystems largely influenced by climate change that modifies element dynamics (AMAP, 2011; IPCC, 2013): e.g., through modifications of hydrological regime related to precipitation and snowpack cover or through the increase of lithogenic pool with permafrost warming. The influence of vegetation on trace element dynamics was already observed, which can manifest in different processes, including atmospheric deposition

interception (e.g., Ilyin et al., 2017), element storage and recycling (e.g., Herndon et al., 2015), and modification of soil properties changing trace element speciation (e.g., Ren et al., 2015). It has been recently reported that Arctic tundra vegetation plays an important role on Hg cycling through accumulation of gaseous elemental Hg from the atmosphere (Obriest et al., 2017). Processes involved, however, are currently not well understood and need more investigation.

In this context, we expect that vegetation in the tundra–taiga transition ecosystem can modify the current and future dynamics of elements coming from local rock dust, regional mining, and long-range atmospheric deposition. More specifically, we hypothesize that lichens and mosses, as well as herbaceous plant species, accelerate the accumulation of elements from the atmosphere to the soil related to their physiological features (higher bioaccumulation and faster turnover, respectively) compared to ligneous species, such as shrubs. The main objective of this study was to determine the spatial distribution of potentially harmful elements in subarctic soils in northern Sweden (Abisko) comparing different land covers (grassland, moor, broad-leaved forest, and peat bog) in order to specifically: (1) identify the occurrence and sources of trace elements in these soils and (2) evaluate the influence of ecosystems on the element distribution.

2. Materials and methods

2.1. Study sites

The study area was located around Abisko Scientific Research Station in northern Sweden (68.3°N), about 200 km north to the Arctic circle (Fig. 1). Four sampling sites, characterized by different land covers, were considered: two located on the east slope of the Njulla Mountain at 975 m a.s.l. (NJU975) and 383 m a.s.l. (NJU383), one on the north-west slope of the Baddosdievvá Mountain at 599 m a.s.l. (BAD599), and one on the south shore of Lake Torneträsk at 363 m a.s.l. (TOR363).

2.1.1. Lithology and soil

All study sites were located in the Scandinavian Mountains characterized by metamorphic lithologies mainly from the Caledonian (490–390 Ma) and Svecofennian (1.85–1.75 Ga) orogenies (Table 1). More specifically, NJU975 and NJU383 were characterized by Cambrian and Ordovician metamorphic bedrocks (phyllite, micaschist, quartzite, metaconglomerate), including limestone deposits. BAD599 also presented metamorphic unit (feldspathic metasandstone, calcareous micaschist, quartzite, phyllite, metaconglomerate, amphibolite, eclogite) dated from the Neoproterozoic. Finally, TOR363 was characterized by a distinct lithology due to its location between an Ediacarian and Cambrian platform sedimentary unit (sandstone, conglomerate, siltstone, shale) and a Palaeoproterozoic lithotectonic unit (granite and pegmatite). Study sites were characterized by acidic organic-rich soils (histosols) that were underlain by a discontinuous permafrost (approximately 4–16 m thick according to the location) with an active layer of 60–80 cm thick during the last decade (Åkerman and Johansson, 2008).

2.1.2. Climate

Abisko is characterized by a cool continental/subarctic climate (Dfc following the Köppen climate classification) with a mean annual air temperature of −0.1 °C and a mean annual precipitation of 330 mm a⁻¹ (averages from 1981 to 2010, Abisko Meteorologic Station NOAA-NCDC). Recent evolution of Abisko climate showed a significant increase in both temperatures and precipitation: modeled rise is about 1.75 °C for annual air temperatures and 69.3 mm a⁻¹ for annual precipitations between 1967 and 2013 (Courault et al., 2015). The prevailing winds were from the south-west (26% as a percentage frequency, 1987–2017, Abisko Meteorologic Station NOAA-NCDC; Fig. 1) and remained unchanged over seasons (34% in fall, 36% in winter, and 22% in spring), excepted in summer where winds come from the north-

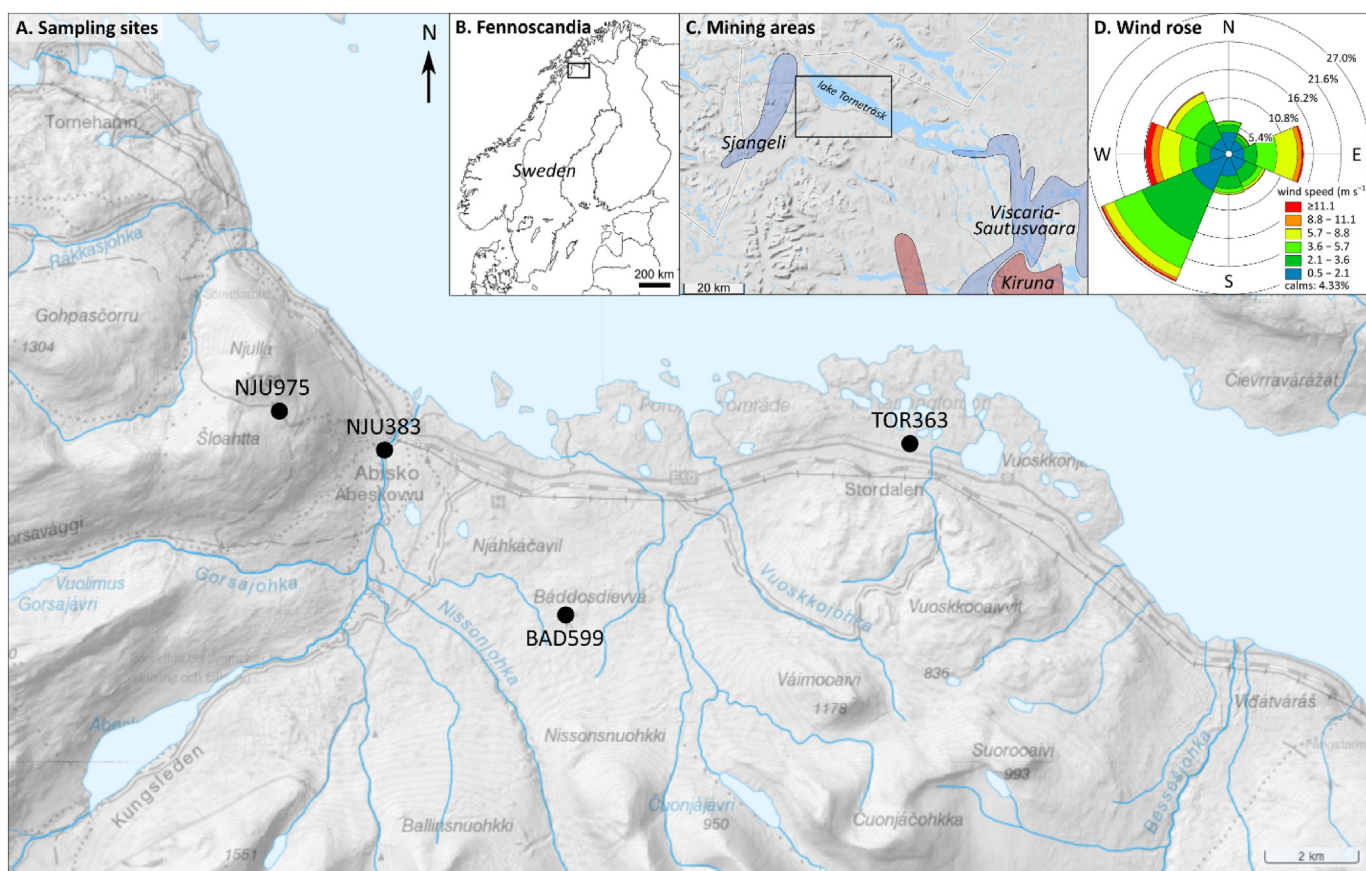


Fig. 1. Location of the four study sites around Abisko Scientific Research Station (www.sgu.se; **A**) in Northern Sweden (**B**). The mining areas were indicated by colored shapes of the regional map (**C**): Cu mines in blue and Fe mines in red (Eilu, 2012). Wind rose is presented for Abisko (1987–2017, Abisko Meteorological Station NOAA-NCDC; **D**). (For interpretation of the references to color in this figure legend, the reader is referred to the web version of this article.)

west (22%). The mean annual wind speeds were 3.46 m s^{-1} (1987–2017, Abisko Meteorological Station NOAA-NCDC).

Based on downscaled reanalysis (CHELSA project; Karger et al., 2017) and interpolated data from the WorldClim 2.0 data base (Fick and Hijmans, 2017), mean annual air temperatures varied from -3.2 to $-0.1 \text{ }^\circ\text{C}$ according to the local topoclimatology (i.e., elevation, slope

steepness, and exposure; Table 1). Average wind speed decelerated from the summits to the Lake Torneträsk (NJU975 to TOR363).

2.1.3. Mining context

Several metallogenic areas, producing base metals (blue shapes in the map) and ferrous metals (red shapes in the map) as far back as

Table 1
Environmental characteristics of the four study sites.

| | NJU975 | BAD599 | NJU383 | TOR363 |
|---|--|---------------------|--|--|
| Latitude/longitude | 68.363°N/18.716°E | 68.317°N/18.867°E | 68.355°N/18.763°E | 68.349°N/19.057°E |
| Elevation (m a.s.l.) ^a | 975 | 599 | 383 | 363 |
| Slope aspect/steepness ^a | SE/ -3.25° | SW/ -1° | ESE/ -2° | N/ -1° |
| Mean annual air temperature (1979–2013; $^\circ\text{C}$) ^b | -3.2 | -1.2 | -0.1 | -0.3 |
| Precipitation (1979–2013; mm a^{-1}) ^b | 602 | 449 | 413 | 402 |
| Average wind speed (1970–2000; m s^{-1}) ^c | 3.2 | 2.7 | 2.5 | 2.3 |
| Bedrock | Mica-rich metamorphic rocks | Calc-silicate rocks | Mica-rich metamorphic rocks | Quartz-feldspar-rich sedimentary rocks and intrusive rocks |
| Soil type | Histosol | Histosol | Histosol | Histosol |
| Soil pH ^d (range) | | | | |
| Organic horizons | 4.3–6.4 | 3.9–4.9 | 4.2–6.4 | 3.8–5.2 |
| Mineral horizons | 5.2–5.9 | 4.9–5.8 | 4.7–6.6 | 5.1 |
| Land cover ^e | Grassland | Moor | Broad-leaved forest | Peat bog |
| Ecological habitat ^f | Moss and lichen tundra (F1.2)/acid alpine and subalpine grassland (E4.3) | Shrub tundra (F1.1) | Broadleaved swamp woodland on acid peat (G1.5) | Raised bog (D1.1) |

^a Based on a 10 m national DEM (geonorge.no).

^b Based on CHELSA project (downscaled model, ERA-Interim climatic analysis; Karger et al., 2017).

^c Based on interpolated data from the WorldClim 2.0 data base (Fick and Hijmans, 2017)

^d $\text{pH}_{\text{CaCl}_2, 0.25 \text{ mM}}$

^e CORINE Land Cover 2012 (European Environment Agency, 2014)

^f EUNIS habitat (Davies et al., 2004)

the 18th century, are located around the study area (Fig. 1; Eilu, 2012). To the west of Abisko, the mining area of Sjangeli (production of Cu, Fe, Pb, Ag, Au, and U) includes two abandoned open pit Cu mines: Kopparåsen (12 km to the North-West) and Sjangeli (28 km to the South-West). In eastern Abisko, two mining areas are close to Kiruna (80 km to the South-East): Viscaria-Sautusvaara mining area that contained large Cu and Fe deposits (production of Cu, Fe, Au, Zn, Ag, and Co) and Kiruna mining area that contained the most important Fe deposit of Europe (production of Fe, Cu, and Au). According to their respective exposure (i.e., east facing for NJU975 and NJU363 vs. north-west facing for BAD599), we expect different mining influences within the study area.

2.1.4. Ecology

Each site is characterized by distinct land cover (grassland, moor, broad-leaved forest, and peat bog; European Environment Agency, 2014) and ecological habitat (Davies et al., 2004; Table 1). Ecosystems were strongly structured by the altitudinal gradient (~1000 m) between the Lake Törnetrask and the summits (Slättatjåkka/Šloahтта and Njulla Mountains). Four bioclimatic belts were identified in the study area: subalpine birch forest, low, middle, and high alpine belt.

Lowest altitudes are characterized by the subalpine forest belt, a forest type mainly structured by *Betula pubescens* ssp. *czerepanovii*. Shrub and herbaceous layer shared vegetal species in common with the northern boreal zone, including additional mountain species: *Empetrum nigrum* ssp. *nigrum*, *Trollius europaeus*, *Angelica archangelica* ssp. *archangelica*, *Pedicularis* sp. Forest undergrowth are made of heath (*Betula nana*, *Vaccinium myrtillus*) or meadow (*Salix* sp., *Rumex* sp., *Alchemilla* sp., *Saussurea alpina*) communities. Meadows soils were generally less acidic and might locally be calcareous in accordance with Caldonian substratum (Carlsson et al., 1999).

The low alpine belt is located up to 600 m a.s.l. and vegetation structure is very dependent on micro-topography (snow cover duration, soil acidity, water availability, and sun and wind exposures). As summer air temperatures dropped, the mountain birch forest-line gradually disappeared and gave way to prostrate shrubs: patches of hydrophilic *Salix* sp., *Betula nana* mats on snow-free areas, mosaics of *Vaccinium uliginosum*, *Empetrum nigrum* ssp. *hermaphroditum*, *Arctostaphylos alpinus*. Species line of *Vaccinium myrtillus* was commonly found as the last extent of the low alpine belt, and thus heavily dependent on the snow cover duration. Grass heaths represented the typical vegetation landscape of the middle alpine belt. Poaceae, Cyperaceae, and Juncaceae were pretty common (*Carex bigelowii*, *Festuca ovina*, *Juncus trifidus*, *Luzula spicata*, etc.), as well as smaller dwarf shrubs (*Salix polaris*, *Phyllodoce caerulea*). In the high alpine belt from 1100 m a.s.l., frost and the almost continuous presence of snow cover prevented vascular plant growth. Plant cover was thus discontinuous. Patches without snow were a favorable habitat for a very few species, such as *Salix herbacea* or *Ranunculus glacialis*. Mats of mosses and lichens were particularly thick (Carlsson et al., 1999).

All along the altitudinal gradient, mires were present where water, sediment, and organic matter were accumulated. These were extended in large flat areas, particularly on Tornetrask banks (Fig. 1). Water table depth structured mire ecosystem: deep at the center, the water depth was progressively replaced with sediments, organic matter, and vegetation such as *Sphagnum* sp. On the edges, the birch forest rapidly disappeared into hydrophilous woody species, grasses, and sedges, largely dependent on water depth in surface, including *Eriophorum vaginatum*, *Rubus chamaemorus*, and *Carex* sp. (Rydin et al., 1999).

2.2. Sampling protocol

The sampling protocol applied for both soils and vegetation was aligned on the Landsat image grid (30 m × 30 m). For representativeness purpose, three pixels (A, B, and C) were sampled along the diagonal

at BAD599, NJU383, and NJU975 (Fig. 2). Only one pixel was considered at TOR363.

2.2.1. Soil sampling

Soils of the study sites were between 30-cm and >100-cm deep. In this work, the top soil (<1 m deep) was considered and collected using an auger in each corner of the pixels (a, c, e, and g), plus a central sampling point P (orange dots, Fig. 2). One sample, or two when differentiated horizons occurred, were subsampled. Based on the organic carbon (OC) content, we distinguished two horizon classes: organic (OC content > 5%) and mineral (OC content < 5%).

2.2.2. Vegetation sampling

The sampling strategy was semi-stratified, taking account both the altitudinal gradient of vegetation landscapes and the limited time of acquisition for floristic and edaphic data (Frontier, 1983). Each 900 m²-pixel was composed of two crossed transects (green lines, Fig. 2), themselves comprising 42 quadrats of 1 m². Two protocols have been followed, according to vegetal physiognomy. For field layer vegetation (<50 cm height), floristic inventories were conducted on vascular plants, mosses, and lichens. Their cover has been estimated by a systematic sampling using a long needle imbedded in the herbaceous layer (every meter). Vegetal species in contact with the needle were the main contributors of the vegetation layer. The cover of each species (*sp*) was computed as follows: $\sum \text{contact}_{sp} \times 100/42$ needle-points (Daget and Godron, 1995). When tree and shrub layers were encountered, the intercept cover protocol was applied for vegetation up to 50 cm height (Canfield, 1941).

To estimate the influence of vegetation on geochemical distribution, percentages of vegetation cover were computed for the five quadrats encompassing each soil sampling achieved (orange dots, Fig. 2). Then, vegetal taxa have been grouped into eight plant functional groups following the tundra ecosystems key, adapted from Walker (2000): lichens, mosses, forbs, graminoids, dwarf shrubs (deciduous and evergreen), shrubs (deciduous and evergreen), and trees (deciduous and evergreen).

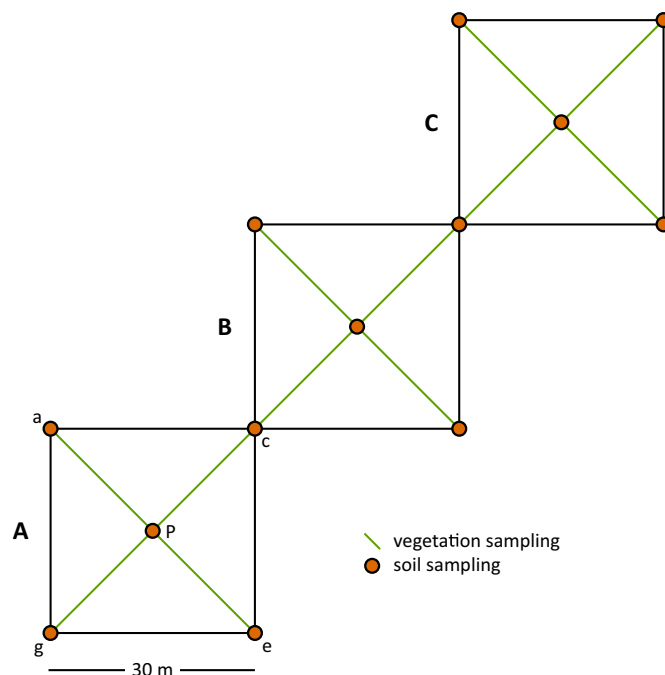


Fig. 2. Sampling protocol for soils and vegetation applied in each study sites considering three pixels (A, B, and C) following the Landsat imagery grid, with the exception of TOR363 where only one pixel was sampled. Soil sampling considered four corner points (a, c, e, and g) and a central point (P) in each pixel.

2.3. Soil sample processing and chemical analyses

Soil samples were dried (<40 °C in an oven for several days), sieved (<2 mm), and ground (<200 µm) using a soil grinder (planetary ball mill PM200, Retsch, Haan, Germany). Soil pH and conductivity were measured in the 0.25 mmol L⁻¹ CaCl₂ extraction solution (solution/soil ratio of 1:10). The total dissolution of the samples was performed using a mixture of suprapure acids (HNO₃ and HF) and H₂O₂. All cleaning and analytical procedures used high purity Milli-Q water (18.2 MΩ cm). Approximately 100 mg of ground soil sample were dissolved using 0.5 mL of 50% HF at 90 °C in a Savillex (Teflon bottle) for 24 h. Then, 1 mL of 65% HNO₃ was added and kept at room temperature for 6 h before adding 1 mL of 30% H₂O₂ for 24 h at 40 °C for evaporation. Finally, we added 1 mL of 65% HNO₃ for 24 h and solutions were diluted with Milli-Q water to obtain a final acid concentration of 2% HNO₃ for ICP analysis. A set of 9 trace elements (As, Cd, Co, Cr, Pb, Sb, Se, Sn, and V) was quantified using ICP–MS Agilent 7500 CE (Agilent Technologies, Santa Clara, CA, USA) at the Alysés platform (Sorbonne Université) and a second set of 6 trace elements (Ba, Cu, Mn, Ni, Sr, and Zn) using ICP–OES Agilent 5100 SVDV (Agilent Technologies, Santa Clara, CA, USA) at the ALIPP6 platform (Sorbonne Université). In parallel, the concentrations of three major elements (Al, Fe, and Ti), considered as geochemical tracers, were measured in bulk soil samples by XRF Niton XL3t (Thermo Scientific, Billerica, MA USA) performed at ISTE P (Sorbonne Université).

Limits of detection (LOD) and limits of quantification (LOQ) were calculated for each element using 3- and 10-times, respectively, the standard deviation determined on the blank samples, with the exception of XRF measurements. LOD were <1000 µg g⁻¹ for Al, <40 µg g⁻¹ for Fe, <20 µg g⁻¹ for Ti, <0.3 µg g⁻¹ for Cu and Ni, <0.2 µg g⁻¹ for Sr and Zn, <0.1 µg g⁻¹ for Ba and Se, <0.02 µg g⁻¹ for Co and Mn, <0.01 µg g⁻¹ for V, <0.005 µg g⁻¹ for As, Cd, Cr, and Sn, <0.002 µg g⁻¹ for Sb, and <0.001 µg g⁻¹ for Pb. We then used (LOD / LOQ)/2 for concentration values below LOQ and LOD/2 for concentration values below LOD.

The procedure performance of the dissolution for ICP–MS and ICP–OES was checked for each series of 35 samples by adding two replicates each of soil and sediment certified materials: LKSD–1, CRM–033, BCR–146, BCR–277, and BCR–320. The average recovery ($C_{\text{measured}}/C_{\text{certified}} \times 100$) was calculated for each analyte: 100 ± 5% for As, Ba, Cd, Cu, Mn, Pb, V, and Zn, 100 ± 10% for Se and Sr, 100 ± 20% for Sn, and 100 ± 30% for Co, Cr, Ni, and Sb. The absence of contamination during the digestion procedure was checked through 2–4 blank samples analyzed per series. A multi-element quality control samples (1 µg L⁻¹ standard) was used every eight samples to correct the analytical deviation of the ICP–MS. Additionally, a control liquid sample (CRM TMDA 64.2) was analyzed at the beginning of each series to check the measurement quality (recovery between 90 and 110%).

In parallel, OC content was measured using a CHNS elemental analyzer (Elementar® vario PYRO cube, Langensfeld, Germany) at the Institut d'écologie et des sciences de l'environnement (CISE platform, iEES, Paris, France). Tyrosine was used as internal analytical standard every four samples and analytical precision was estimated to 0.2%.

2.4. Data processing and statistical analyses

2.4.1. Enrichment factor

The enrichment factor (EF; Chester and Stoner, 1973; Vieira et al., 2004) was calculated for each trace and major element (X) in organic soil horizon class samples using Al as normalized element and mineral horizon class samples as reference material:

$$EF = \frac{(X/Al)_{\text{organic}}}{(X/Al)_{\text{mineral}}}$$

A comparison between Al and Ti as normalized element was made: it should be noted that values with Al represented the maximum EFs.

2.4.2. Statistical analyses

All statistics were performed using R 3.5.1 (R Foundation for Statistical Computing, Vienna, Austria) and RStudio 1.1.453 (RStudio Inc., Boston, Massachusetts, USA). Statistically significant differences were tested using the non-parametric Kruskal–Wallis test ($\alpha = 0.05$) and a post-hoc Dunn test ($\alpha = 0.05$) using the *dunn.test* package.

To identify the relationships between trace and major elements, a principal component analysis (PCA) was performed with *FactoMineR* and *factoextra* packages on element concentrations after centered log-ratio transformation using *rgr* package (*clr* function). Contributions of element sources were estimated using a non-negative matrix factorization (NMF)—an innovative statistical method recently used in environmental geochemistry (Christensen et al., 2018)—with *NMF* package (Gaujoux and Seoighe, 2010). The number of factors to best fit the model was determined to be four. Finally, a partial least squares (PLS) regression was performed using *plsdepot* package (*plsreg2* function) to determine the influence of environmental variables (vegetation and soil parameters) on trace and major element distribution in organic horizon classes.

3. Results and discussions

3.1. Occurrence of trace and major elements in subarctic soils

3.1.1. Concentration levels of Abisko area soils

Concentrations of trace and major elements were measured in both organic (OC content > 5%) and mineral (OC content < 5%) soil horizon classes from Abisko (Table 2). Values showed a wide range of median concentrations from Sb (0.14 µg g⁻¹) to Fe (20,300 µg g⁻¹) in organic horizon classes and from Cd (0.23 µg g⁻¹) to Al (104,000 µg g⁻¹) in mineral horizon classes. This concentration variability between elements is frequent in natural Arctic and subarctic environments, such as in soil (Reimann et al., 2015), snow (Shevchenko et al., 2017), water (Manasyrov et al., 2015), or vegetation (Wojtuń et al., 2013). For each considered element, concentrations were widely distributed: from 10- (Pb) to >1000-fold (Ni) between the highest and the lowest values. Mineral horizon classes showed higher median values compared to organic ones, particularly for Al, Sr, Ba, Mn, Cr, Sn, V, and Co (between 3- and >4-fold). The opposite trend was only observed for Cu and Cd.

Compared to data from Nord-Trøndelag (Central Norway), a region also belonging to the Fennoscandian range (Reimann et al., 2015), the present data set showed generally higher median element concentrations in both organic and mineral horizon classes (Table 2): on average, 4- and 7-fold higher at Abisko, respectively. The maxima were observed for Ba and Sr that could be explained by distinct lithologies between the two regions (West and East slope of the Scandinavian Mountain). This was particularly obvious for V, Ti, Al, Fe, and Cr in organic horizon classes (from 5- to 10-fold higher) and for Ba, Sr, Al, Cd, and Se for mineral horizon classes (up to 32-fold). It should be mentioned that this difference can be largely attributed to the preparation methods for chemical analyses: total HF dissolution in the present study (except for Al, Fe, and Ti analyzed on the solid soil fraction by XRF) vs. aqua regia dissolution in Reimann et al. (2015). Some elements showed opposite trend in organic soil horizon classes with lower median concentrations observed at Abisko: Pb, Sb, Cd, Zn, and Sn. We suggest that either Abisko was less atmospherically-influenced by these trace elements due to lower atmospheric depositions, or that Abisko's distinct surface environment (such as vegetation) influenced metal and metalloid recycling (Kabata-Pendias, 2004).

3.1.2. Comparison of concentrations across subarctic ecosystems

We compared concentrations measured in both organic and mineral soil horizon classes between the different study sites. Four groups of elements were identified according to their spatial and vertical distribution patterns (Fig. 3). The first group included Al, Co, Cr, Fe, Mn, Ni, Ti, and V (illustrated by Ti; Fig. 3A) and showed statistically significantly higher concentrations in mineral horizon classes. This element

Table 2

Summary of trace and major element concentrations in organic (OC content > 5%) and mineral (OC content < 5%) soil horizon classes and comparison with soil concentrations from Nord-Trøndelag (Central Norway).

| | Soil concentration in Abisko ($\mu\text{g g}^{-1}$) | | | | Soil concentration in Central Norway ^a ($\mu\text{g g}^{-1}$) | |
|----|---|--------------|--------------------------|----------------|--|---------------------------|
| | Organic horizon (n = 44) | | Mineral horizon (n = 21) | | Median in organic horizon | Median in mineral horizon |
| | Median | Range | Median | Range | | |
| Al | 16,700.00 | 2170–95,900 | 104,000.00 | 80,100–128,000 | 2030.00 | 11,787.00 |
| As | 1.67 | 0.27–11.0 | 3.13 | 1.23–5.51 | 0.81 | 1.48 |
| Ba | 128.00 | 19.1–632 | 480.00 | 81.5–605 | 36.00 | 15.00 |
| Cd | 0.24 | <0.01–2.92 | 0.23 | 0.09–0.67 | 0.51 | 0.03 |
| Co | 6.12 | 1.02–202 | 18.90 | 6.05–28.6 | 1.48 | 6.14 |
| Cr | 15.20 | 1.38–78.2 | 55.10 | 36.6–100 | 3.03 | 26.00 |
| Cu | 20.90 | 3.28–204 | 18.00 | 2.54–97.9 | 7.86 | 13.00 |
| Fe | 20,300.00 | 2570–136,000 | 42,800.00 | 26,000–74,600 | 3003.00 | 19,419.00 |
| Mn | 224.00 | 2.80–1910 | 820.00 | 83.4–2270 | 58.00 | 167.00 |
| Ni | 8.03 | <0.23–108 | 21.30 | 5.73–130 | 3.23 | 14.00 |
| Pb | 6.53 | 1.76–19.5 | 14.20 | 6.65–18.3 | 27.00 | 6.61 |
| Sb | 0.14 | <0.01–1.60 | 0.40 | 0.04–3.64 | 0.33 | 0.04 |
| Se | 2.06 | 0.39–15.1 | 2.94 | 0.39–7.70 | 0.90 | <0.50 |
| Sn | 0.58 | 0.01–2.30 | 1.90 | 1.40–2.58 | 0.75 | 0.44 |
| Sr | 44.40 | 14.6–214 | 181.00 | 25.8–256 | 30.00 | 6.87 |
| Ti | 1510.00 | 163–4470 | 4170.00 | 3660–7830 | 161.00 | 1032.00 |
| V | 28.30 | 2.95–138 | 91.40 | 63.5–273 | 2.91 | 31.00 |
| Zn | 25.90 | 0.68–179 | 69.70 | 20.2–193 | 38.00 | 27.00 |

^a Reimann et al. (2015).

association was generally related to a lithogenic origin (Halbach et al., 2017; Kabata-Pendias, 1993). The concentrations reported in BAD599 were statistically significantly higher compared to other study sites. Because of the complex silicate-rich local bedrock, it remains difficult to clearly identify the rock type and/or minerals responsible for such high concentrations specifically observed in BAD599.

The second group of elements included Pb, Sb, Sn, and Zn (illustrated by Sn; Fig. 3B). These elements presented a similar pattern as previously observed (i.e., statistically significantly higher concentrations in mineral horizon classes), with the exception of BAD599 that did not show the same extremely high values in mineral horizon classes (compared to Ti for example, Fig. 3A). This indicates the absence of important mineral

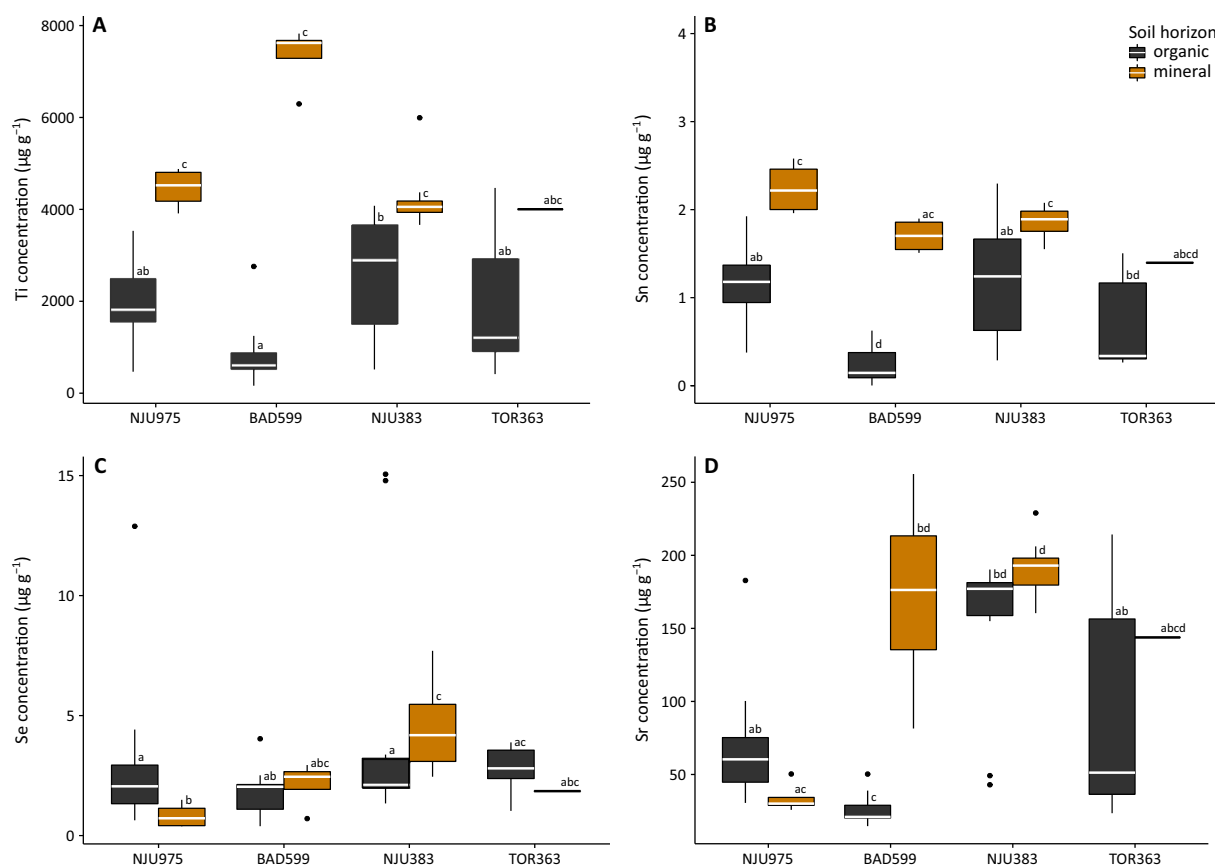


Fig. 3. Concentrations of Ti (A), Sn (B), Se (C), and Sr (D) in both organic (gray, n = 44) and mineral (brown, n = 21) soil horizon classes for the four study sites in Abisko. Letters represent statistically significant differences using Kruskal-Wallis and Dunn post-hoc tests ($p < 0.05$). (For interpretation of the references to color in this figure legend, the reader is referred to the web version of this article.)

contribution related to the BAD599 lithology. Moreover, some of these elements were well known to be part of the long-range atmospheric deposition even in the Arctic, such as Pb and Zn (McConnell and Edwards, 2008; Shevchenko et al., 2003).

The third group of elements included As, Cd, Cu, and Se (illustrated by Se; Fig. 3C) and showed clearly distinct pattern compared to the two previous groups. Concentrations in mineral horizon classes were either lower (NJU975), or higher (NJU383) than those measured in organic horizon classes, while concentrations were constant across the study sites in organic horizon classes. This implies the absence of major bedrock influence for these elements. Dynamics of As, Cu, and Se are known to be largely controlled by soil redox and pH (Masscheleyn et al., 1991; Shaheen et al., 2013), parameters largely variables in organic-rich and temporarily water-saturated soils. These elements are also influenced by biological activities, such as methylation processes (Carbonell et al., 1998; Winkel et al., 2015). Cadmium was already observed abundantly in surface soil horizons because of its strong dependence on atmospheric deposition (Halbach et al., 2017).

Finally, the fourth group of elements included two alkaline earth metals: Ba and Sr (illustrated by Sr; Fig. 3D). This association presented a very specific behavior with high concentrations in mineral horizon classes in BAD599, NJU383, and possibly TOR363 (only one data point in TOR363). These two elements are well known to be chemically similar to Ca, facilitating substitutions (Lucas et al., 1990). Indeed, BAD599 was characterized by a calc-silicate bedrock and NJU383 was overhung by a limestone deposit 300–400 m higher. A dilution process may explain the fact that Sr and Ba were weakly concentrated in organic soil horizon classes from BAD599, while NJU383 should be affected by carbonate-rich dust coming from the top of the mountain. The influence of carbonates, however, was limited given the acidic soil pH (Table 1).

3.2. Sources of trace and major elements in subarctic soils

3.2.1. Enrichment of elements

The EF is frequently used to identify natural vs. anthropogenic origins (Agnan et al., 2015; Reimann and de Caritat, 2005). In this study, we only considered organic soil horizon classes and compared to mineral ones for identifying surface inputs (i.e., atmospheric deposition, vegetation, etc.) after lithologic normalization. This method makes study sites comparable by eliminating the local lithology influence.

Results, presented for each site on a logarithmic scale, were compared to the reference value of 1 (Fig. 4): enrichment if $EF > 1$ and depletion if $EF < 1$. Because EFs calculated using Al as normalized element were higher compared to those using Ti, we used the threshold of $EF = 2$ for considering an enrichment.

Antimony was the only element showing a depletion in both BAD599 and TOR363 (on average close to 0.1 and up to <0.01 for some samples). This may result from either an Al enrichment in organic horizon classes (that could induce depletion of other elements), or a Sb-rich lithology attenuating the low surface inputs in these two aforementioned sites. Six elements (Cr, Mn, Ni, Sn, Ti, and V), most of them previously included in the first group (Fig. 3A), did not show enrichment ($EF < 2$) in the four study sites (with the exception of Mn in NJU383 and Cr and V in TOR363). This corroborates the main lithogenic origin for these elements. Considering the lithology normalization, Ba and Sr only showed enrichment in NJU975 that probably reflects a local atmospheric deposition of carbonate-rich dust from the nearby limestone deposit despite the absence of such minerals in the soil profile. This also illustrates the lack of Ba and Sr anomalies in BAD599 and NJU383, as observed in Fig. 3D.

The lowest EF values were observed in BAD599, while Fe was slightly enriched in BAD599 and TOR363 (EF between 3 and 4). In the same way, average EFs of Co, Pb, and Zn were >3 , with important site heterogeneity. The highest enrichments were observed in NJU975 and BAD599, and to a lesser extent in TOR363 (up to $EF > 10$). This illustrates the large influence of surface processes, even for Co previously characterized as lithogenic element (Fig. 3A). Overall, the specific enrichment of Cu, Fe, and Pb observed in BAD599 can be related to direct atmospheric influences from Sjangeli mining area (from southwestern prevailing winds). Conversely, NJU975 presented the highest enrichments of Co, Mn, and Zn that we may attribute to a regional influence of Viscaria mining area (from eastern winds).

Finally, As, Cd, Cu, and Se showed the highest enrichments (up to >100 for Cd and Cu). Statistically significant differences were evidenced between sites, with the same trend for As, Cu, and Se: $BAD599 > TOR363 > NJU975 > NJU383$. This indicates distinct intensities for surface processes responsible for the presence of these chemicals (factor of 8–10 for As and Se and up to 44 for Cu between BAD599 and NJU383). Cadmium, however, only presented lower EFs in TOR363 (median EF of 4), while median EF reached 6–10 for the three other sites. Since the

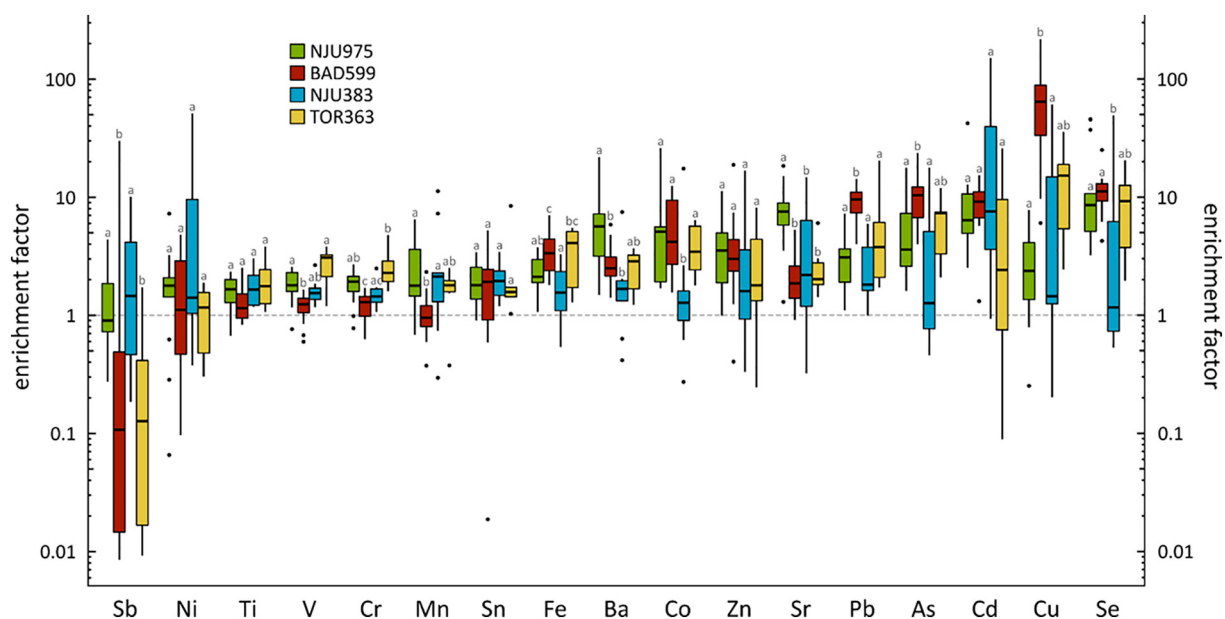


Fig. 4. Enrichment factor of trace and major elements in organic soil horizons normalized to Al and mineral soil horizons of the same study sites. The dash gray line indicates the enrichment factor of 1. Letters represent statistically significant differences using Kruskal-Wallis and Dunn post-hoc tests ($p < 0.05$).

EF cannot fully distinguish the origins of elements (e.g., mining, long-range atmospheric deposition, vegetation), we suggest the use of multivariate analyses to identify the distinct sources and quantify their contribution.

3.2.2. Principal component analysis: covariance between elements

A PCA was thus performed on trace and major element concentrations measured in Abisko soil samples to identify the covariance between elements. The first three components explained 64% of the data variance. We represented both observations (soil samples) and variables (elements) in biplot diagrams (Fig. 5). Principal component 1 (28% of the data variance) allowed the grouping of Al, Cr, Sn, Ti, and V with positive scores and As, Cd, Cu, and Se with negative ones (Fig. 5A). This principal component was mainly driven by soil horizon classes considered (Fig. 5B): mineral samples with positive scores vs. organic samples with negative scores. This demonstrates that the nature of horizon class represented the first driver for the distribution of trace and major elements. We previously discussed the lithogenic origin of the first group (Fig. 3A), including Al, Cr, Ti, and V. Surprisingly, Fe was not included in principal component 1, despite its high concentrations in mineral samples (Table 2), as frequently observed in the literature (Reimann et al., 2007). At the opposite end, As, Cd, Cu, and Se were already highlighted as part of the third group related to surface processes, including both biological influence and atmospheric deposition (Fig. 3C).

Principal component 2 (24% of the data variance) associated As, Fe, and Pb with positive scores and Mn, Ni, and Sb with negative scores

(Fig. 5A). This principal component seemed to be partly controlled by the location: in organic horizon class samples (i.e., negative scores of principal component 1), BAD599 and TOR363 were mostly located in the positive scores while NJU383 and NJU975 were mostly in the negative scores (Fig. 5C). This grouping was not observed in mineral horizon classes and probably resulted from surface processes, such as different atmospheric inputs. Indeed, as previously discussed, geographical features may explain this site differentiation: NJU383 and NJU975 were both located on the same mountain slope with similar eastern exposure, promoting the influence of East mining areas (e.g., Viscaria-Sautusvaara). Due to the low influence of Fe, we assume that Kiruna mining area was either too far, or not adequately located to atmospherically transport contaminants to the study area. Conversely, BAD599, and to a lesser extent TOR363, were under the influence of South-West winds (e.g., Sjangeli mining area), which are sources of Cu, Fe, and Pb, among other elements, resulting in the presence of these chemicals in principal component 2. It should be noted that this mixed source of Fe may explain the absence of Fe in the lithogenic element group.

Finally, principal component 3 (12% of the data variance) only highlighted two elements previously grouped together: Ba and Sr (Fig. 5D). We assume that this resulted from carbonate-rich dust in BAD599 and NJU383, as previously discussed (Fig. 3D). Considering the acidic soil pH (mineral soil pH ≤ 6.6), we assume that this source was limited in the overall geochemical composition. In the next section, we present the NMF analysis to evaluate the contribution of the various sources to each single element measured.

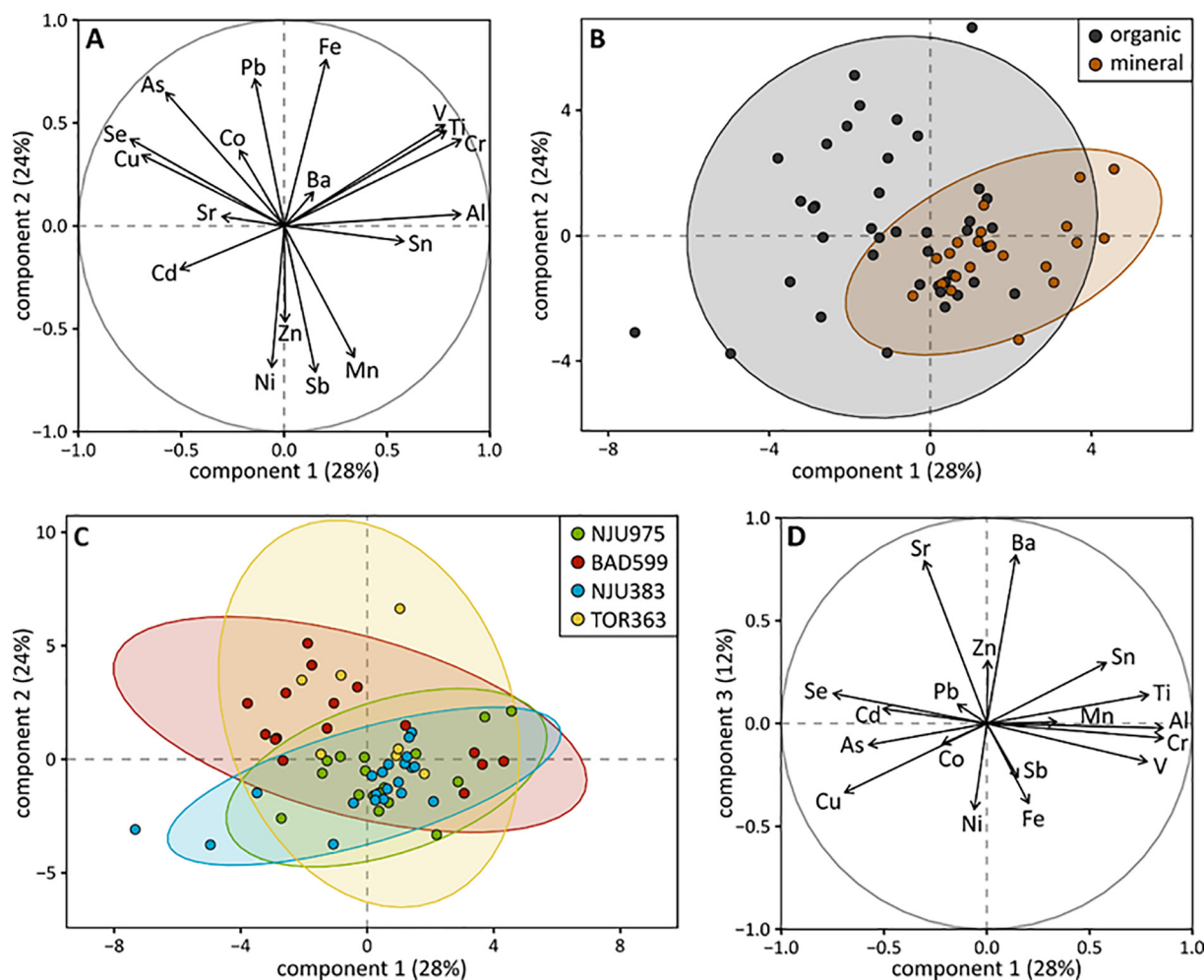


Fig. 5. Principal component analysis of log-ratio transformed trace and major element concentrations in soil samples collected at Abisko ($n = 61$): representation of elements for components 1 vs. 2 (A) and components 1 vs. 3 (D) and representation of observations by soil horizon class (B) and by study site (C) for components 1 vs. 2.

3.2.3. Non-negative matrix factorization: contribution of different sources

The NMF, recently applied to environmental geochemistry (Christensen et al., 2018), was performed to identify the contribution of different sources to trace and major element concentrations. The relative contribution of the four factors selected are represented for each element (Fig. 6A) and sampling site by soil horizon class (Fig. 6B). For clarity in the graphical representations, we reordered the factors following the discussion.

First, factor 1 contributed significantly (>35%) to Al, Cr, Fe, Sn, Sr, Ti, and V (Fig. 6A). With high prevalence in mineral horizon classes (on average, 42 vs. only 17% in organic ones; Fig. 6B), this factor likely represented a strong lithogenic source relatively homogeneously distributed in the study area (Halbach et al., 2017), confirming the results obtained by EFs (Fig. 4) and PCA (Fig. 5). The highest contribution in mineral horizon classes was observed in BAD599 at 60%, corroborating the low EFs observed in this site for Cr, Mn, V, and Ti (Fig. 4).

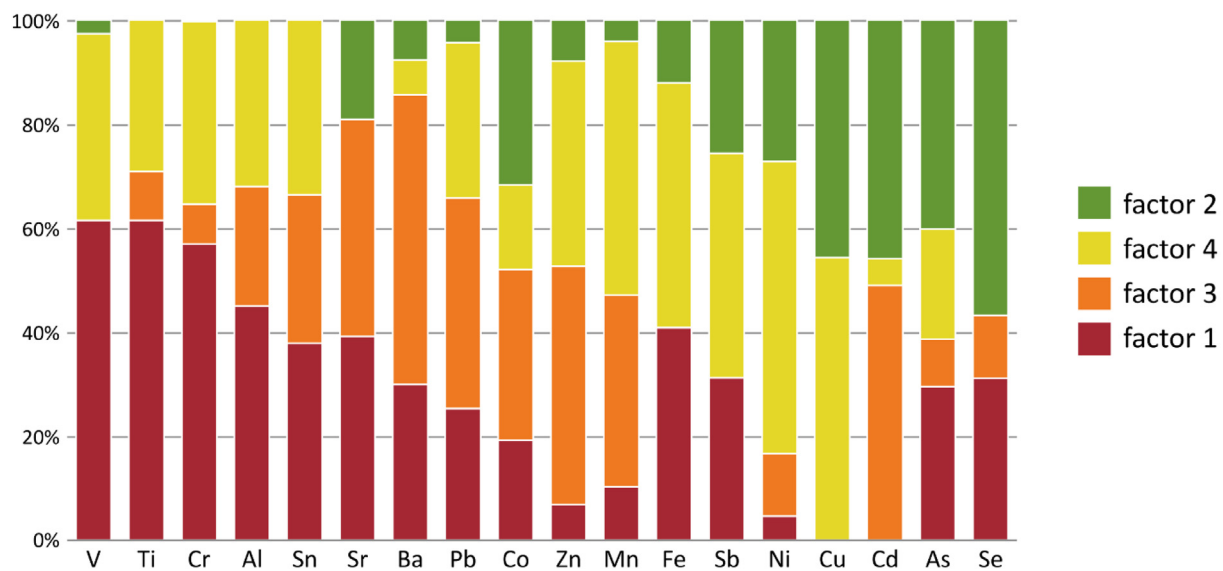
Factor 3 showed a high contribution (>35%) to Ba, Cd, Pb, Mn, Sr, and Zn, including an important inter-site heterogeneity with the highest contribution in NJU383 (36%) and the lowest one in BAD599 (9%). Surprisingly, it was almost equally distributed between organic and mineral horizon classes in all study sites. This illustrates a site specificity that might result from different lithologies between Njulla (NJU383 and NJU975) and Baddosdievvá (BAD599) Mountains. The complexity

of geological terrain of the study area cannot confirm this assumption. However, the important contrast between sites could result from distinct atmospheric inputs: Njulla Mountain sites were mainly influenced by eastern winds (e.g., from Viscaria mining area). Besides, considering the chemical association (e.g., Cd, Pb, Zn), we may suggest that factor 3 also constituted a source for global long-range atmospheric deposition (Nygård et al., 2012). We thus attribute this factor to a mixed origin mainly driven by both regional mining influence and global atmospheric deposition.

Factor 4 contributed importantly (>35%) to Cr, Cu, Fe, Mn, Ni, Sb, V, and Zn. The contribution decreased in the following order: NJU975 > BAD599 > NJU383 > TOR363. On average, mineral horizon classes had higher contribution than organic ones (28 vs. 22%, respectively). In NJU975, factor 4 accounted for almost half of the total contribution in mineral horizon classes. Considering the geochemical composition (Cu, Fe, Pb), we attribute factor 4 to a local mining influence (e.g., from southwestern Sjangeli mining area), also illustrated in the positive scores of the principal component 2 (Fig. 5A). Since the contribution was important in mineral horizon classes, we assume that factor 4 was also associated with the local lithology particularly enriched in several base metals (Reimann et al., 2015).

Finally, factor 2 showed dominant contribution (>35%) to As, Cd, Cu, and Se. This factor contributed 38% in organic horizon classes (mainly in

A. By element



B. By site

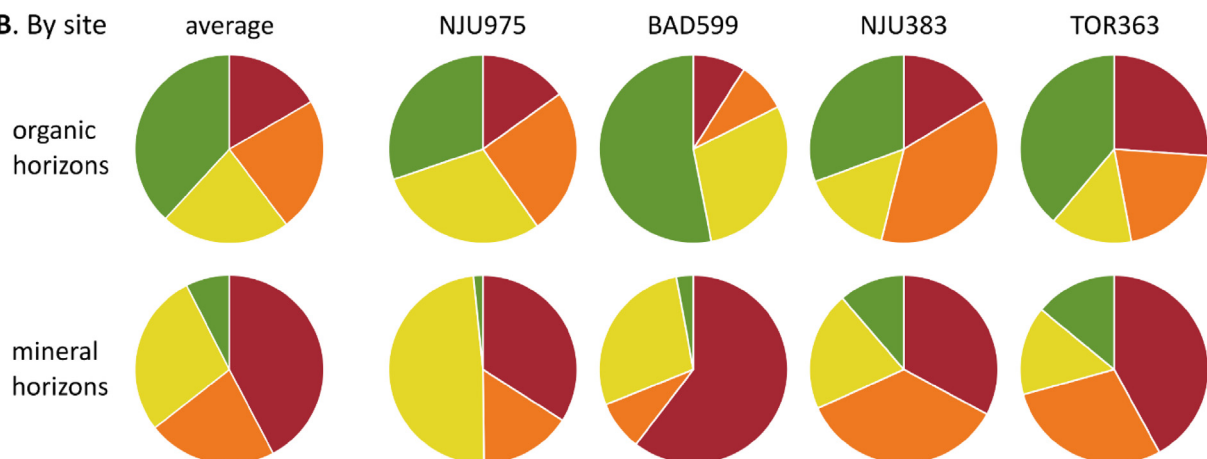


Fig. 6. Non-negative matrix factorization of trace and major element concentrations in soil samples collected at Abisko ($n = 61$): contribution of the four factors for each element (A) and sampling site by soil horizon class (B). Each factor represents distinct source: lithogenic (factor 1), surface (factor 2), mixed (factor 3), and mining (factor 4).

BAD599 and TOR363 with 53 and 39%, respectively) and only 7% in mineral ones. The differing contribution between the horizon classes could suggest surface process influence being captured by factor 2 (Figs. 3C and 5A). All of these elements were also reported to be accumulated in organic horizons in European boreal forests due to their atmospheric deposition and their strong link to soil organic matter (Gustafsson and Johnsson, 1992; Räisänen et al., 1997). To better constrain the influence of vegetation on element distribution, we now propose a covariance analysis between geochemical and vegetation data using a PLS regression.

3.3. Influence of vegetation on trace and major element distribution

Vegetation was sampled in each study site, corresponding to distinct ecosystems and land covers according to decreasing altitude: grassland (NJU975), moor (BAD599), broad-leaved forest (NJU383), and peat bog (TOR363). Following the Walker (2000) classification for Arctic and subarctic vegetation, we adapted and simplified the classes to: trees, shrubs, dwarf shrubs, graminoids, forbs, mosses, and lichens. We then distinguished deciduous and evergreen vegetation for trees, shrubs, and dwarf shrubs. Vegetation classes were heterogeneously distributed across the sites with dominance of dwarf shrubs (42%) in BAD599, forbs (42%) in NJU383, and graminoids (87%) in TOR363 (Table 3). In NJU975, dwarf shrubs and graminoids were almost equal proportions (22–26%). Trees were only found in NJU383 at a paltry 5% for both deciduous (*Betula pubescens* ssp. *czerepanovii* and *Sorbus aucuparia*) and evergreen (*Juniperus communis*) species. Shrubs and dwarf shrubs were mostly found in NJU975 and BAD599. Only deciduous shrubs (*Betula nana* and *Salix phylicifolia*) were collected, while both deciduous (e.g., *Vaccinium uliginosum*, *Rubus saxatilis*, *Salix herbacea*) and evergreen (e.g., *Empetrum nigrum* ssp. *hermaphroditum*, *Vaccinium vitis-idaea*, *Dryas octopetala*, *Loiseleuria alpinum*) species were reported for dwarf shrubs. The graminoid species collected at Abisko belonged to Cyperaceae (e.g., *Eriophorum vaginatum*, *Eleocharis acicularis*, *Carex vesicaria*), Juncaceae (e.g., *Luzula* sp.), and Poaceae; the species *Carex vesicaria* was specifically found in TOR363 with an important frequency. Forbs were highly found in NJU383, including *Epilobium angustifolium*, *Trollius europaeus*, *Saussurea alpina*, *Myosotis* sp., *Viola biflora*, and *Paris quadrifolia*. Finally, mosses were mostly found in NJU383 (21%) and lichens (e.g., *Cetraria*, *Cladonia*) in NJU975 and BAD599 (16% in both cases).

We performed a PLS regression combining geochemical data (first three PCA components and four NMF factors) as dependent variables with environmental data (frequency of vegetation classes and soil pH and conductivity) as independent variables. The data set consists of 37 observations collected in each sampling point (9–13 per study site, except for TOR363). To better understand the influence of vegetation, we only considered organic soil horizon classes thereby limiting any

lithogenic inputs. The first two axes represented 53% of the data variance for independent variables and 23% for dependent variables.

The first axis of the correlation circle showed factor 3 (i.e., mixed influence, including lithogenic, regional mining, and long-range atmospheric deposition) with positive scores and principal component 2 (i.e., local mining influence) with negative ones (Fig. 7A). Surprisingly, factor 4 (i.e., local mining influence) was not correlated to principal component 2. This can result from the opposite influence for principal components (positive scores vs. negative ones), whereas factors corresponded to single sources. Vegetation classes that were influenced by the first axis were: trees and forbs (positive scores) and shrubs, dwarf shrubs, and lichens (negative scores). Because of the limited representativeness of trees in the study area, it is difficult to correctly interpret their role in the geochemical distribution. Moreover, in NJU383, pixels A and B differed from pixel C by forb and bryophyte proportions, and not by tree proportions. This indicates that positive scores of the first axis were mainly driven by forbs. The first axis clearly differentiated NJU383 with positive scores from BAD599 and NJU975 with negative scores (Fig. 7B), corresponding to their distinct vegetation classes. The fact that NJU975 and NJU383 are presented diametrically despite their geochemically similar inputs (Figs. 5 and 6) supports the limited bedrock effect along the first axis. The annual activity of forbs may contribute to the recycling of lithogenic elements (factors 1 and 3). Conversely, perennial shrubs and dwarf shrubs present a higher bioaccumulation (Wojtuń et al., 2013), and therefore a lower recycling because of the element retention. When differentiating deciduous and evergreen species, results showed similar covariances as previously observed (data not shown). We attribute this finding to a physiological effect (i.e., perennial vs. annual) rather than a leaf biomass production effect (i.e., deciduous vs. evergreen). Finally, despite similar phytosociological behaviors in the ecosystems, lichens and bryophytes, two classes of vegetation well known to efficiently accumulate trace elements that permit to accurately evaluate atmospheric deposition (Agnan et al., 2015; Steinnes et al., 2003), were opposed along the first axis, probably resulting from distinct bioaccumulated elements between these two vegetation classes (Gandois et al., 2014).

The second axis of the correlation circle showed factor 2 (i.e., surface processes), and to a lesser extent factor 4 (i.e., local mining influence), with negative scores and principal component 3 (i.e., calcareous lithology) with low positive scores (Fig. 7A). Despite both lichens and bryophytes were slightly influenced along the negative scores, soil pH appeared as the main driver of the second axis, controlled by the sampling sites: the more acidic soil pH were observed in BAD599, TOR363, pixels A and B of NJU383, and pixel C of NJU975 (Fig. 7B). This illustrates the higher element solubility in more acidic soils, promoting their mobilization (Shaheen et al., 2013). Conversely, the less acidic soils retained trace elements such as As, Cd, and Cu. Selenium was also associated to factor 4 while its adsorption decreased with increasing pH (Söderlund et al., 2016). Thus, soil pH does not seem to be the only parameter that controls the dynamics of these elements. This observation implies more complex surface processes that we cannot identify in this study.

Following the results observed here, two hypotheses could be formulated: (1) vegetation influenced the distribution through distinct bioaccumulation and recycling processes (Shahid et al., 2017) or (2) soil geochemistry influenced the distribution of vegetation as an edaphic variable (Thuiller, 2013). Both hypotheses seem possible following the two PLS regression axes (axes 1 and 2, respectively). Unfortunately, the influence of vegetation on trace element distribution is poorly documented in the literature, particularly in Arctic and subarctic ecosystems. We also assume that vegetation may be impacted by the altitudinal gradient (from 363 to 975 m a.s.l.) that likely masked the edaphic influence. However, considering the findings from this study and the quick changes in Arctic and subarctic vegetation composition recently observed at Abisko (Callaghan et al., 2013), we expect modifications in trace element cycling. This is of particular concern since shrubs, one of the main vegetation groups that was correlated with

Table 3
Proportions (in %) of vegetation classes following the adapted Walker (2000) classification in the four study sites (in bold). Both deciduous and evergreen were identified for trees, shrubs, and dwarf shrubs (in italic).

| | NJU975 | BAD599 | NJU383 | TOR363 |
|--------------|-----------|-----------|-----------|-----------|
| Trees | – | – | 5 | – |
| Deciduous | – | – | 2 | – |
| Evergreen | – | – | 3 | – |
| Shrubs | 10 | 10 | 1 | 2 |
| Deciduous | <i>10</i> | <i>10</i> | <i>1</i> | <i>2</i> |
| Evergreen | – | – | – | – |
| Dwarf shrubs | 26 | 42 | 13 | 5 |
| Deciduous | <i>6</i> | <i>16</i> | <i>6</i> | <i>2</i> |
| Evergreen | <i>20</i> | <i>26</i> | <i>7</i> | <i>5</i> |
| Graminoids | 22 | 19 | 14 | 87 |
| Forbs | 11 | 1 | 42 | 1 |
| Mosses | 15 | 12 | 21 | 3 |
| Lichens | 16 | 16 | 4 | 2 |

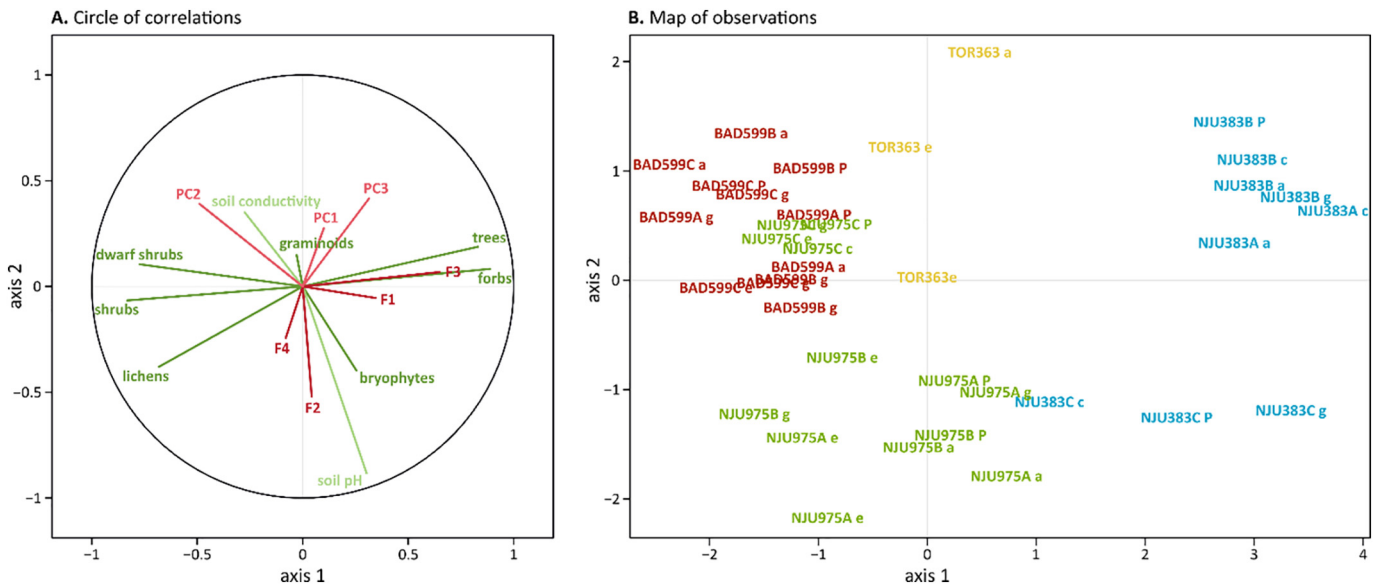


Fig. 7. Partial least squares regression using geochemical data (the first three principal components from the PCA [PC1, PC2, and PC3] and the four factors from the NMF [F1, F2, F3, and F4]) as dependent variables (red) and environmental data (vegetation classes according to the Walker (2000) classification and soil pH and conductivity) as independent variables (green): circle of correlations (A) and map of observations (B). Only organic soil horizon classes were considered ($n = 37$). (For interpretation of the references to color in this figure legend, the reader is referred to the web version of this article.)

trace elements, are known to be currently expanding with climate change (Myers-Smith et al., 2015). Because herbivore mammals in the high latitudes, such as reindeer, are largely dependent on vegetation as intake, such modifications may impact the whole trophic network (Pacyna et al., 2019). These preliminary results, however, need to be confirmed, and trace element dynamics in the Arctic and subarctic environments, better characterized in further research.

4. Conclusions

In this study, we measured trace and major element concentrations in both organic and mineral soil horizon classes from four different subarctic land covers: grassland, moor, broad-leaved forest, and peat bog. The main objectives were to: (1) identify the occurrence and sources of elements and (2) evaluate the influence of vegetation on the element spatial distribution. Results showed non-negligible concentrations that partially resulted from natural regional enrichments. Several trends were observed according to the study site and the considered soil horizon class. The association between elements showed a strong influence of the soil horizon class: lithogenic (Al, Cr, Ti) vs. surface influenced (As, Cu, Se) elements. Atmospheric influences, including contamination from local and regional mines (Cu, Fe, Mn, Ni, Pb), as well as long-range atmospheric transport (Cd, Zn), were observed in surface organic horizon classes. Every source identified was not exclusive for each trace and major element: a non-negative matrix factorization allowed quantification of contribution of each single source. To our knowledge, this study is the first to combine geochemical with ecological data in high latitude environments to evaluate the covariance between vegetation and element concentrations using a partial least square regression. Forbs and shrubs/dwarf shrubs were highlighted as the main vegetation classes controlling the geochemical dynamics likely due to their annual vs. perennial activities, respectively. In addition, the control of geochemical dynamics by soil pH could be evidenced for As, Cu, and Se. We thus expect that the evolution of vegetation in Arctic and subarctic regions related to climate change may modify the dynamics of trace elements, either directly by accumulating elements from the atmosphere to the soil, or indirectly by modifying the soil pH, and up to the whole trophic network through herbivore mammals. Further research is therefore required to confirm the findings of the present study.

Acknowledgements

Thanks to ENVEXX team for sampling (Hugo Potier, Juliette Grosset, Déborah Harlet, Thomas Kabani, Samantha Launay, Thibault Lemaître-Basset, and Giulia Sardano). We also thank Emmanuel Aubry, Véronique Vaury and Lancelot Pinta for analytical support, Benoit Caron for ICP-OES (ALIPP6), Florence le Cornec and Irina Djouaev for ICP-MS (ALIZE), and Laurence Le Callonnec and Nathalie Labourdette for XRF. The funding was provided by Sorbonne Universités (Collège des licences, ENVEXX project) and element analysis by TETRISÉ project (supported by the Needs Environment 2012 program, CNRS-ANDRA-IRSN-EDF). We also would like to acknowledge the Abisko Research Station for their hospitality and the scientific support. We thank Jimmy Ong for his proofreading of the manuscript. We also thank two anonymous reviewers for their valuable comments to improve the manuscript.

References

- Acosta Navarro, J.C., Varma, V., Riipinen, I., Seland, Ø., Kirkevåg, A., Struthers, H., Iversen, T., Hansson, H.-C., Ekman, A.M.L., 2016. Amplification of Arctic warming by past air pollution reductions in Europe. *Nat. Geosci.* 9, 277–281. <https://doi.org/10.1038/ngeo2673>.
- Agnan, Y., Séjalon-Delmas, N., Probst, A., 2014. Origin and distribution of rare earth elements in various lichen and moss species over the last century in France. *Sci. Total Environ.* 487, 1–12. <https://doi.org/10.1016/j.scitotenv.2014.03.132>.
- Agnan, Y., Séjalon-Delmas, N., Claustres, A., Probst, A., 2015. Investigation of spatial and temporal metal atmospheric deposition in France through lichen and moss bioaccumulation over one century. *Sci. Total Environ.* 529, 285–296. <https://doi.org/10.1016/j.scitotenv.2015.05.083>.
- Åkerman, H.J., Johansson, M., 2008. Thawing permafrost and thicker active layers in subarctic Sweden. *Permafrost. Periglac. Process.* 19, 279–292. <https://doi.org/10.1002/ppp.626>.
- AMAP, 2011. *Snow, Water, Ice and Permafrost in the Arctic (SWIPA): Climate Change and the Cryosphere*. Arctic Monitoring and Assessment Programme (AMAP), Oslo.
- AMAP, 2018. *AMAP Assessment 2018: Biological Effects of Contaminants on Arctic Wildlife and Fish*. Arctic Monitoring and Assessment Programme (AMAP), Oslo.
- Barbante, C., Veyseyre, A., Ferrari, C., Van De Velde, K., Morel, C., Capodaglio, G., Cescon, P., Scarponi, G., Boutron, C., 2001. Greenland snow evidence of large scale atmospheric contamination for platinum, palladium, and rhodium. *Environ. Sci. Technol.* 35, 835–839. <https://doi.org/10.1021/es000146y>.
- Beck, P.S.A., Goetz, S.J., 2011. Satellite observations of high northern latitude vegetation productivity changes between 1982 and 2008: ecological variability and regional differences. *Environ. Res. Lett.* 6, 045501. <https://doi.org/10.1088/1748-9326/6/4/045501>.
- Berner, L.T., Beck, P.S.A., Bunn, A.G., Goetz, S.J., 2013. Plant response to climate change along the forest-tundra ecotone in northeastern Siberia. *Glob. Chang. Biol.* 19, 3449–3462. <https://doi.org/10.1111/gcb.12304>.

- Callaghan, T.V., Werkman, B.R., Crawford, Robert.M.M., 2002a. The tundra-taiga interface and its dynamics: concepts and applications. *Ambio Special Report* 12, 6–14.
- Callaghan, T.V., Crawford, R.M.M., Eronen, M., Hofgaard, A., Payette, S., Rees, W.G., Skre, O., Sveinbjörnsson, B., Vlassova, T.K., Werkman, B.R., 2002b. The dynamics of the tundra-taiga boundary: an overview and suggested coordinated and integrated approach to research. *Ambio Special Report* 12, 3–5.
- Callaghan, T.V., Jonasson, C., Thierfelder, T., Yang, Z., Hedenas, H., Johansson, M., Molau, U., Van Bogaert, R., Michelsen, A., Olofsson, J., Gwynn-Jones, D., Bokhorst, S., Phoenix, G., Bjerke, J.W., Tommervik, H., Christensen, T.R., Hanna, E., Koller, E.K., Sloan, V.L., 2013. Ecosystem change and stability over multiple decades in the Swedish subarctic: complex processes and multiple drivers. *Philos. Trans. R. Soc. B Biol. Sci.* 368, 20120488. <https://doi.org/10.1098/rstb.2012.0488>.
- Canfield, R.H., 1941. Application of the line interception method in sampling range vegetation. *J. For.* 39, 388–394. <https://doi.org/10.1093/jof/39.4.388>.
- Carbonell, A.A., Aarabi, M.A., DeLaune, R.D., Gambrell, R.P., Patrick Jr, W.H., 1998. Arsenic in wetland vegetation: availability, phytotoxicity, uptake and effects on plant growth and nutrition. *Sci. Total Environ.* 217, 189–199. [https://doi.org/10.1016/S0048-9697\(98\)00195-8](https://doi.org/10.1016/S0048-9697(98)00195-8).
- Carlsson, B.A., Karlsson, P.S., Svensson, B.M., 1999. 6. Alpine and subalpine vegetation. In: Rydin, H., Snoeijis, P., Diekmann, M. (Eds.), *Swedish Plant Geography, Acta Phytogeographica Suecica*. Svenska Västgeografiska Sällskapet, Uppsala, pp. 75–89.
- Chapin, F.S.I., Matson, P.A., Vitousek, P., 2011. *Principles of Terrestrial Ecosystem Ecology*. Springer, New York.
- Chester, R., Stoner, J.H., 1973. Pb in particulates from the lower atmosphere of the Eastern Atlantic. *Nature* 245, 27–28. <https://doi.org/10.1038/245027b0>.
- Christensen, E.R., Steinnes, E., Eggen, O.A., 2018. Anthropogenic and geogenic mass input of trace elements to moss and natural surface soil in Norway. *Sci. Total Environ.* 613–614, 371–378. <https://doi.org/10.1016/j.scitotenv.2017.09.094>.
- Courault, R., Cohen, M., Ronchail, J., 2015. Régimes de circulation atmosphérique, impact du changement climatique et variation démographique des rennes dans le nord de la Scandinavie. *Modélisations et Variabilités: Actes Du XXVIII^e Colloque de l'Association Internationale de Climatologie*. Presented at the XXVIII Colloque de l'Association Internationale de Climatologie, Liège, Belgium, pp. 123–128.
- Daget, P., Godron, M., 1995. *Pastoralisme. Troupeaux, espaces et sociétés*. Hatier, Aupelf, Uref, Universités francophones, Paris.
- Davies, C.E., Moss, D., Hill, M.O., 2004. *EUNIS Habitat Classification Revised 2004*. European Topic Centre on Nature Protection and Biodiversity, Paris.
- Dietz, R., Riget, F., Cleemann, M., Aarkrog, A., Johansen, P., Hansen, J., 2000. Comparison of contaminants from different trophic levels and ecosystems. *Sci. Total Environ.* 245, 221–231. [https://doi.org/10.1016/S0048-9697\(99\)00447-7](https://doi.org/10.1016/S0048-9697(99)00447-7).
- Eilu, P. (Ed.), 2012. *Mineral Deposits and Metallogeny of Fennoscandia, Special Paper/ Geological Survey of Finland. Geological Survey of Finland, Espoo*.
- European Environment Agency, 2014. *CLC2012: Addendum to CLC2006 Technical Guidelines*. Office for Official Publications of the European Communities, Luxembourg.
- Evenset, A., Christensen, G.N., Carroll, J., Zaborska, A., Berger, U., Herzke, D., Gregor, D., 2007. Historical trends in persistent organic pollutants and metals recorded in sediment from Lake Ellasjøen, Bjørnøya, Norwegian Arctic. *Environ. Pollut.* 146, 196–205. <https://doi.org/10.1016/j.envpol.2006.04.038>.
- Fedele, L., Plant, J.A., Vivo, B.D., Lima, A., 2008. The rare earth element distribution over Europe: geogenic and anthropogenic sources. *Geochem. Explor. Environ. Anal.* 8, 3–18. <https://doi.org/10.1144/1467-7873/07-150>.
- Fick, S.E., Hijmans, R.J., 2017. WorldClim 2: new 1-km spatial resolution climate surfaces for global land areas. *Int. J. Climatol.* 37, 4302–4315. <https://doi.org/10.1002/joc.5086>.
- Frontier, S., 1983. *Stratégies d'échantillonnage en écologie*. Masson, Paris.
- Gamberg, M., Braune, B., Davey, E., Elkin, B., Hoekstra, P.F., Kennedy, D., Macdonald, C., Muir, D., Nirwal, A., Wayland, M., Zeeb, B., 2005. Spatial and temporal trends of contaminants in terrestrial biota from the Canadian Arctic. *Sci. Total Environ.* 351–352, 148–164. <https://doi.org/10.1016/j.scitotenv.2004.10.032>.
- Gamberg, M., Cuyler, C., Wang, X., 2016. Contaminants in two West Greenland caribou populations. *Sci. Total Environ.* 554–555, 329–336. <https://doi.org/10.1016/j.scitotenv.2016.02.154>.
- Gandois, L., Agnan, Y., Leblond, S., Séjalon-Delmas, N., Le Roux, G., Probst, A., 2014. Use of geochemical signatures, including rare earth elements, in mosses and lichens to assess spatial integration and the influence of forest environment. *Atmos. Environ.* 95, 96–104. <https://doi.org/10.1016/j.atmosenv.2014.06.029>.
- Gaujoux, R., Seoighe, C., 2010. A flexible R package for nonnegative matrix factorization. *BMC Bioinformatics* 11, 367. <https://doi.org/10.1186/1471-2105-11-367>.
- Gustafsson, J.P., Johnsson, L., 1992. Selenium retention in the organic matter of Swedish forest soils. *J. Soil Sci.* 43, 461–472. <https://doi.org/10.1111/j.1365-2389.1992.tb00152.x>.
- Halbach, K., Mikkelsen, Ø., Berg, T., Steinnes, E., 2017. The presence of mercury and other trace metals in surface soils in the Norwegian Arctic. *Chemosphere* 188, 567–574. <https://doi.org/10.1016/j.chemosphere.2017.09.012>.
- Herndon, E.M., Jin, L., Andrews, D.M., Eissenstat, D.M., Brantley, S.L., 2015. Importance of vegetation for manganese cycling in temperate forested watersheds. *Glob. Biogeochem. Cycles* 29, <https://doi.org/10.1002/2014GB004858> (2014GB004858).
- Ilyin, I., Rozovskaya, O., Travnikov, O., Aas, W., 2017. Assessment of heavy metal transboundary pollution on regional and national scales, transition to the new EMEP grid (EMEP status report 2/2017). Meteorological Synthesizing Centre-East & Norwegian Institute for Air Research, Moscow - Kjeller.
- IPCC, 2013. *Climate Change 2013: The Physical Science Basis. Contribution of the Working Group I to the Fifth Assessment Report of the Intergovernmental Panel on Climate Change*. Cambridge University Press, Cambridge - New York.
- Ju, J., Masek, J.G., 2016. The vegetation greenness trend in Canada and US Alaska from 1984–2012 Landsat data. *Remote Sens. Environ.* 176, 1–16. <https://doi.org/10.1016/j.rse.2016.01.001>.
- Kabata-Pendias, A., 1993. Behavioural properties of trace metals in soils. *Appl. Geochem., Environmental Geochemistry* 8, 3–9. [https://doi.org/10.1016/S0883-2927\(09\)80002-4](https://doi.org/10.1016/S0883-2927(09)80002-4).
- Kabata-Pendias, A., 2004. *Soil-Plant Transfer of Trace Elements—An Environmental Issue*. Geoderma, Biogeochemical Processes and the Role of Heavy Metals in the Soil Environment. vol. 122, pp. 143–149. <https://doi.org/10.1016/j.geoderma.2004.01.004>.
- Kabata-Pendias, A., 2010. *Trace Elements in Soils and Plants*. 4th ed. CRC Press.
- Karger, D.N., Conrad, O., Böhner, J., Kawohl, T., Kreft, H., Soria-Auza, R.W., Zimmermann, N.E., Linder, H.P., Kessler, M., 2017. Climatologies at high resolution for the earth's land surface areas. *Sci. Data* 4, 170122. <https://doi.org/10.1038/sdata.2017.122>.
- Klassen, R.A., Douma, S., Rencz, A.N., 2010. Environmental and human health risk assessment for essential trace elements: considering the role for geoscience. *J. Toxicol. Environ. Health A* 73, 242–252. <https://doi.org/10.1080/15287390903340906>.
- Law, K.S., Stohl, A., 2007. Arctic air pollution: origins and impacts. *Science* 315, 1537–1540. <https://doi.org/10.1126/science.1137695>.
- Lucas, J., El Faleh, E.M., Prevot, L., 1990. Experimental study of the substitution of Ca by Sr and Ba in synthetic apatites. *Geol. Soc. Lond. Spec. Publ.* 52, 33–47. <https://doi.org/10.1144/GSL.SP.1990.052.01.04>.
- Manasyov, R.M., Vorobyev, S.N., Loiko, S.V., Kritzkov, I.V., Shirokova, L.S., Shevchenko, V.P., Kirpotin, S.N., Kulizhsky, S.P., Kolesnichenko, L.G., Zemtsov, V.A., Sinkin, V.V., Pokrovsky, O.S., 2015. Seasonal dynamics of organic carbon and metals in thermokarst lakes from the discontinuous permafrost zone of western Siberia. *Biogeosciences* 12, 3009–3028. <https://doi.org/10.5194/bg-12-3009-2015>.
- Masscheleyn, P.H., Delaune, R.D., Patrick, W.H., 1991. Arsenic and selenium chemistry as affected by sediment redox potential and pH. *J. Environ. Qual.* 20, 522–527. <https://doi.org/10.2134/jeq1991.00472425002000030004x>.
- McConnell, J.R., Edwards, R., 2008. Coal burning leaves toxic heavy metal legacy in the Arctic. *Proc. Natl. Acad. Sci.* 105, 12140–12144. <https://doi.org/10.1073/pnas.0803564105>.
- Myers-Smith, I.H., Elmendorf, S.C., Beck, P.S.A., Wilkening, M., Hallinger, M., Blok, D., Tape, K.D., Rayback, S.A., Macias-Fauria, M., Forbes, B.C., Speed, J.D.M., Boulanger-Lapointe, N., Rixen, C., Lévesque, E., Schmidt, N.M., Baittinger, C., Trant, A.J., Hermanutz, L., Collier, L.S., Dawes, M.A., Lantz, T.C., Weijers, S., Jørgensen, R.H., Buchwal, A., Buras, A., Naito, A.T., Ravolainen, V., Schaepman-Strub, G., Wheeler, J.A., Wipf, S., Guay, K.C., Hik, D.S., Vellend, M., 2015. Climate sensitivity of shrub growth across the tundra biome. *Nat. Clim. Chang.* 5, 887–891. <https://doi.org/10.1038/ncclimate2697>.
- Nygård, T., Steinnes, E., Royset, O., 2012. Distribution of 32 elements in organic surface soils: contributions from atmospheric transport of pollutants and natural sources. *Water Air Soil Pollut.* 223, 699–713. <https://doi.org/10.1007/s11270-011-0895-5>.
- Obriet, D., Agnan, Y., Jiskra, M., Olson, C.L., Colegrove, D.P., Hueber, J., Moore, C.W., Sonke, J.E., Helmig, D., 2017. Tundra uptake of atmospheric elemental mercury drives Arctic mercury pollution. *Nature* 547, 201–204. <https://doi.org/10.1038/nature22997>.
- Pacyna, A.D., Frankowski, M., Koziół, K., Węgrzyn, M.H., Wietrzyk-Pelka, P., Lehmann-Konera, S., Polkowska, Z., 2019. Evaluation of the use of reindeer droppings for monitoring essential and non-essential elements in the polar terrestrial environment. *Sci. Total Environ.* 658, 1209–1218. <https://doi.org/10.1016/j.scitotenv.2018.12.232>.
- Räisänen, M.L., Kshulina, G., Bogatyrev, I., 1997. Mobility and retention of heavy metals, arsenic and sulphur in podzols at eight locations in northern Finland and Norway and the western half of the Russian Kola Peninsula. *J. Geochem. Explor.* 59, 175–195. [https://doi.org/10.1016/S0375-6742\(97\)00014-9](https://doi.org/10.1016/S0375-6742(97)00014-9).
- Reimann, C., de Caritat, P., 2005. Distinguishing between natural and anthropogenic sources for elements in the environment: regional geochemical surveys versus enrichment factors. *Sci. Total Environ.* 337, 91–107.
- Reimann, C., Arnoldussen, A., Englmaier, P., Filzmoser, P., Finne, T.E., Garrett, R.G., Koller, F., Nordgulen, O., 2007. Element concentrations and variations along a 120-km transect in southern Norway - anthropogenic vs. geogenic vs. biogenic element sources and cycles. *Appl. Geochem.* 22, 851–871. <https://doi.org/Article>.
- Reimann, C., Schilling, J., Roberts, D., Fabian, K., 2015. A regional-scale geochemical survey of soil O and C horizon samples in Nord-Trøndelag, Central Norway: geology and mineral potential. *Appl. Geochem.* 61, 192–205. <https://doi.org/10.1016/j.apgeochem.2015.05.019>.
- Ren, Z.-L., Tella, M., Bravin, M.N., Comans, R.N.J., Dai, J., Garnier, J.-M., Sivry, Y., Doelsch, E., Straathof, A., Benedetti, M.F., 2015. Effect of dissolved organic matter composition on metal speciation in soil solutions. *Chem. Geol.* 398, 61–69. <https://doi.org/10.1016/j.chemgeo.2015.01.020>.
- Romanovsky, V.E., Smith, S.L., Christiansen, H.H., 2010. Permafrost thermal state in the polar Northern Hemisphere during the international polar year 2007–2009: a synthesis. *Permafrost. Periglacial Process.* 21, 106–116. <https://doi.org/10.1002/ppp.689>.
- Rydin, H., Sjörs, H., Löfroth, M., 1999. 7. Mires. In: Rydin, H., Snoeijis, P., Diekmann, M. (Eds.), *Swedish Plant Geography, Acta Phytogeographica Suecica*. Svenska Västgeografiska Sällskapet, Uppsala, pp. 91–112.
- Shaheen, S.M., Tsadilas, C.D., Rinklebe, J., 2013. A review of the distribution coefficients of trace elements in soils: influence of sorption system, element characteristics, and soil colloidal properties. *Adv. Colloid Interf. Sci.* 201–202, 43–56. <https://doi.org/10.1016/j.cis.2013.10.005>.
- Shahid, M., Dumat, C., Khalid, S., Schreck, E., Xiong, T., Niazi, N.K., 2017. Foliar heavy metal uptake, toxicity and detoxification in plants: a comparison of foliar and root metal uptake. *J. Hazard. Mater.* 325, 36–58. <https://doi.org/10.1016/j.jhazmat.2016.11.063>.
- Shevchenko, V., Lisitzin, A., Vinogradova, A., Stein, R., 2003. Heavy metals in aerosols over the seas of the Russian Arctic. *Sci. Total Environ.* 306, 11–25. [https://doi.org/10.1016/S0048-9697\(02\)00481-3](https://doi.org/10.1016/S0048-9697(02)00481-3).
- Shevchenko, V.P., Pokrovsky, O.S., Vorobyev, S.N., Krivkov, I.V., Manasyov, R.M., Politov, N.V., Kopysov, S.G., Dara, O.M., Auda, Y., Shirokova, L.S., Kolesnichenko, L.G., Zemtsov, V.A., Kirpotin, S.N., 2017. Impact of snow deposition on major and trace element concentrations and elementary fluxes in surface waters of the Western Siberian Lowland

- across a 1700 km latitudinal gradient. *Hydrol. Earth Syst. Sci.* 21, 5725–5746. <https://doi.org/10.5194/hess-21-5725-2017>.
- Shiyatov, S.G., Terent'ev, M.M., Fomin, V.V., Zimmermann, N.E., 2007. Altitudinal and horizontal shifts of the upper boundaries of open and closed forests in the Polar Urals in the 20th century. *Russ. J. Ecol.* 38, 223–227. <https://doi.org/10.1134/S1067413607040017>.
- Söderlund, M., Virkanen, J., Holgersson, S., Lehto, J., 2016. Sorption and speciation of selenium in boreal forest soil. *J. Environ. Radioact.* 164, 220–231. <https://doi.org/10.1016/j.jenvrad.2016.08.006>.
- Steinnes, E., Lierhagen, S., 2018. Geographical distribution of trace elements in natural surface soils: atmospheric influence from natural and anthropogenic sources. *Appl. Geochem.* 88, 2–9. <https://doi.org/10.1016/j.apgeochem.2017.03.013>.
- Steinnes, E., Berg, T., Sjobakk, T.E., 2003. Temporal trends in long-range atmospheric transport of heavy metals to Norway. *J. Phys. IV Proc.* 107, 1271–1273. <https://doi.org/10.1051/jp4:20030532>.
- Thuiller, W., 2013. On the importance of edaphic variables to predict plant species distributions - limits and prospects. *J. Veg. Sci.* 24, 591–592. <https://doi.org/10.1111/jvs.12076>.
- Tyler, G., Pahlsson, A.-M.B., Bengtsson, G., Bååth, E., Tranvik, L., 1989. Heavy-metal ecology of terrestrial plants, microorganisms and invertebrates: a review. *Water Air Soil Pollut.* 47, 189–215. <https://doi.org/10.1007/BF00279327>.
- Ulrich, B., Pankrath, J., 1983. *Effects of Accumulation of Air Pollutants in Forest Ecosystems*. Springer, Dordrecht.
- Vieira, B.J., Freitas, M.C., Rodrigues, A.F., Pacheco, A.M.G., Soares, P.M., Correia, N., 2004. Element-enrichment factors in lichens from Terceira, Santa Maria and Madeira Islands (Azores and Madeira archipelagoes). *J. Atmos. Chem.* 49, 231–249. <https://doi.org/ProceedingsPaper>.
- Walker, D.A., 2000. Hierarchical subdivision of Arctic tundra based on vegetation response to climate, parent material and topography. *Glob. Chang. Biol.* 6, 19–34. <https://doi.org/10.1046/j.1365-2486.2000.06010.x>.
- Winkel, L., Vriens, B., Jones, G., Schneider, L., Pilon-Smits, E., Bañuelos, G., 2015. Selenium cycling across soil-plant-atmosphere interfaces: a critical review. *Nutrients* 7, 4199–4239. <https://doi.org/10.3390/nu7064199>.
- Wojtuń, B., Samecka-Cymerman, A., Kolon, K., Kempers, A.J., Skrzypek, G., 2013. Metals in some dominant vascular plants, mosses, lichens, algae, and the biological soil crust in various types of terrestrial tundra, SW Spitsbergen, Norway. *Polar Biol.* 36, 1799–1809. <https://doi.org/10.1007/s00300-013-1399-0>.